

Probing the electrode-polymer interface in conjugated polymer devices with surface-enhanced Raman scattering

Dongbo Li, Nicholas J. Borys, and John M. Lupton

Citation: *Appl. Phys. Lett.* **100**, 141907 (2012); doi: 10.1063/1.3701278

View online: <http://dx.doi.org/10.1063/1.3701278>

View Table of Contents: <http://apl.aip.org/resource/1/APPLAB/v100/i14>

Published by the [American Institute of Physics](http://www.aip.org).

Related Articles

Improved and color tunable electroluminescence from n-ZnO/HfO₂/p-GaN heterojunction light emitting diodes
Appl. Phys. Lett. **100**, 233502 (2012)

Study of field driven electroluminescence in colloidal quantum dot solids
J. Appl. Phys. **111**, 113701 (2012)

Annealed InGaN green light-emitting diodes with graphene transparent conductive electrodes
J. Appl. Phys. **111**, 114501 (2012)

Noniterative algorithm for improving the accuracy of a multicolor-light-emitting-diode-based colorimeter
Rev. Sci. Instrum. **83**, 053115 (2012)

Effects of lateral current injection in GaN multi-quantum well light-emitting diodes
J. Appl. Phys. **111**, 103120 (2012)

Additional information on *Appl. Phys. Lett.*

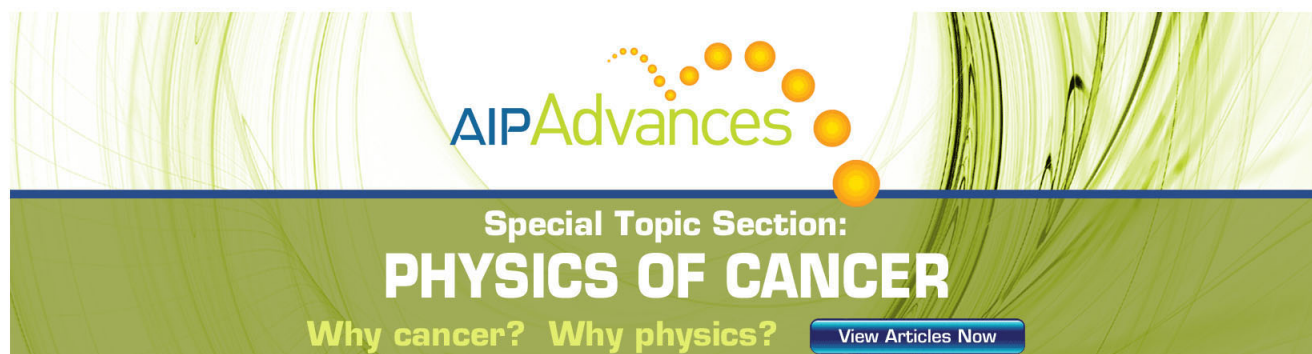
Journal Homepage: <http://apl.aip.org/>

Journal Information: http://apl.aip.org/about/about_the_journal

Top downloads: http://apl.aip.org/features/most_downloaded

Information for Authors: <http://apl.aip.org/authors>

ADVERTISEMENT



AIP Advances

Special Topic Section:
PHYSICS OF CANCER

Why cancer? Why physics? [View Articles Now](#)

Probing the electrode-polymer interface in conjugated polymer devices with surface-enhanced Raman scattering

Dongbo Li, Nicholas J. Borys,^{a)} and John M. Lupton

Department of Physics and Astronomy, University of Utah, Salt Lake City, Utah 84112, USA

(Received 24 January 2012; accepted 13 March 2012; published online 6 April 2012)

A crucial consideration in organic devices is the role of the interface between a metal electrode and the active polymer material. Here, we use the conjugated polymer poly[2-methoxy-5-(2-ethylhexyl-oxy)-1,4-phenylene-vinylene] (MEH-PPV) with model gold and silver electrodes to perform surface-enhanced Raman scattering (SERS) on the metal-MEH-PPV interface. We observe significant differences between the SERS spectra on the two metals, which we assign to conformational changes of the phenyl rings within the polymer. The difference between gold and silver interfaces can be removed upon thermal annealing, suggesting structural relaxation. Resonance Raman spectra of the two interfaces are identical, implying that the overall conformation of the polymer backbone which supports the pi-electron transition remains unaffected by the different metals. SERS is uniquely sensitive to the interfacial metal/organic layer and provides an important *in situ* tool to optimizing organic device structures. © 2012 American Institute of Physics. [<http://dx.doi.org/10.1063/1.3701278>]

Optoelectronic devices with active layers derived from conjugated polymers such as light emitting diodes, photovoltaics, and thin film transistors have made significant practical advancements over the last decade.¹ However, significant challenges in regards to efficiency and stability still remain for such devices, and one such critical issue is an accurate understanding of the composition, structure, and functionality of the many interfaces within these devices.^{2,3} In particular, the interface between a polymer and a metal electrode is almost ubiquitous in polymer-based devices and is suspected to play an important role in their overall performance and stability.⁴ Accordingly, significant attention has been focused on the conformation and energetic alignment of polymers and molecules at this interface.^{4,5}

Optical spectroscopy techniques are facile tools for characterizing polymer-based devices⁶⁻⁸ and can be used to probe non-pristine interfaces that are likely to occur in a production environment.⁹ In particular, Raman scattering, where the vibrational modes of a molecule are mapped out through the inelastic scattering of light, is capable of elucidating subtle structural and chemical differences in molecular systems and has been successfully utilized to probe important changes^{10,11} and degradation effects¹²⁻¹⁴ in organic thin films and device structures. An extension of Raman scattering is surface-enhanced Raman scattering (SERS) where the plasmonic modes of nanostructured metal are used to enhance the Raman process by several orders of magnitude¹⁵ enabling sensitivities reaching the detection of single molecules.^{16,17} The plasmonic enhancement is primarily a near-field electromagnetic effect and thus localizes the measurement to within only a few nanometers of the metal nanostructures, making it an ideal tool to study interfacial effects. As with conventional Raman, SERS has been used to probe polymer films in a device structure to gain information on

the polymer structure in multilayer devices,¹⁸ the effects of device degradation,¹⁹ the differences in preparation conditions for poly(3,4-ethylenedioxythiophene) (PEDOT), a common hole-injecting material,²⁰ and the effects of metallic electrodes on benzene molecules.²¹

Here, we report the use of model electrodes fabricated from gold or silver as SERS substrates to characterize the polymer-metal interface, further illustrating the potential for SERS to be used as an *in situ* tool for probing an operating device. Using poly[2-methoxy-5-(2-ethylhexyl-oxy)-1,4-phenylene-vinylene] (MEH-PPV) as a model polymer film, we find that gold electrodes induce a conformational change at the metal interface as is evident in an additional band in the SERS spectrum that is not present in the Raman spectrum of the bulk film. In contrast, the SERS spectrum of the interface between MEH-PPV and a silver electrode retains nearly the same features as a Raman spectrum of the bulk film, indicating only a weak interfacial interaction in comparison to gold.

All of the devices in this work were fabricated on clean glass cover slips. The silver and gold films, which serve as the model electrodes, were prepared by thermal evaporation at a vacuum of 10^{-6} mbar. Careful characterization revealed that the best Raman enhancement occurred for ~ 9 nm thick films grown at a rate of 1 \AA/s for both silver and gold. We note that although the overall intensity of the SERS signal varied, the relative intensities of the observed peaks were independent of film thickness. Atomic force microscopy (AFM) characterization of the films was conducted on an Asylum Research MFP-3D microscope by scanning the surface in tapping mode with a silicon nitride tip. Solutions of MEH-PPV (American Dye Source) dissolved in chlorobenzene at a concentration of 1 mg/mL were spin-cast at a speed of 2000 r.p.m. , for 60 s yielding a polymer film that is approximately 100 nm thick. The film that was used to determine the bulk MEH-PPV Raman spectrum was prepared by drop-casting the MEH-PPV solution on a glass substrate,

^{a)} Author to whom correspondence should be addressed. Electronic mail: nborys@physics.utah.edu.

which was then allowed to dry for 30 min. All of the preparation procedures were conducted in a glove box under a nitrogen atmosphere at room temperature. After preparation, the samples were removed from the glove box for the Raman and SERS characterization, which were performed on a scanning confocal Raman microscope (Alpha300R from WITec) with a 1.4 NA objective. Continuous wave (CW) illumination at 785 nm from a Ti:sapphire laser pumped by an Argon ion laser was used for off-resonant excitation at incident powers of ~ 10 mW, while CW illumination at 532 nm from a diode laser was used for resonant excitation at a power of ~ 2 mW. The scattered light was collected by the same microscope objective, spectrally filtered to remove the excitation light, and then focused onto a $100\ \mu\text{m}$ optical fiber coupled to a spectrometer. All of the Raman measurements were performed in ambient conditions at room temperature.

Figure 1 compares the Raman spectrum of a bulk MEH-PPV film (Fig. 1(a)) to the SERS spectra of MEH-PPV at the interfaces of both silver (Fig. 1(b)) and gold (Fig. 1(c)) films.

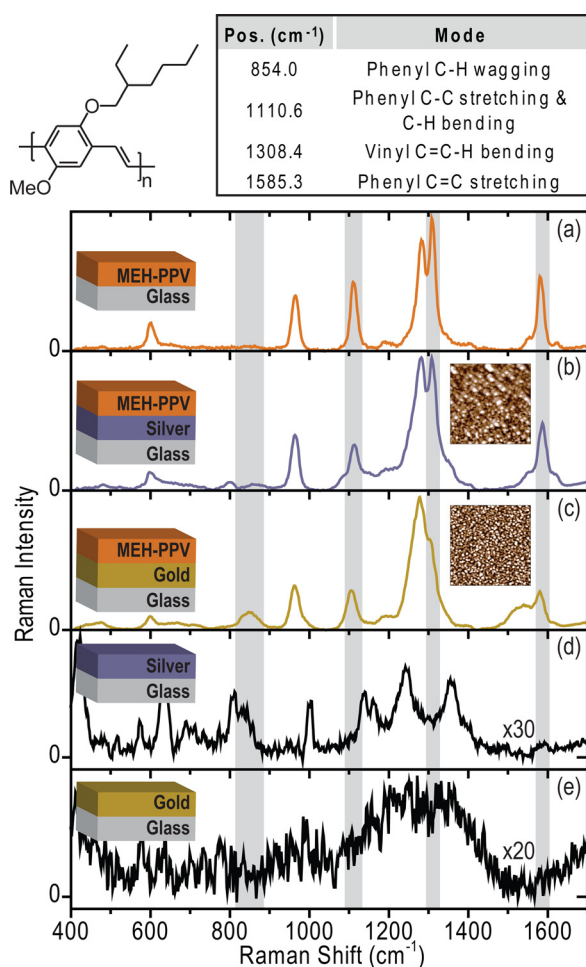


FIG. 1. Raman spectra of MEH-PPV in the bulk and on gold and silver electrodes. At the top, the chemical structure of MEH-PPV and the assignments of selected vibrational modes are shown. The Raman spectrum of a bulk MEH-PPV film (a) is similar to the SERS spectrum of MEH-PPV on a silver film (b) but shows notable differences to the SERS spectrum of MEH-PPV on a gold layer (c). The gray shading marks the spectral positions listed in the above table. The background signals for the silver film (d) and gold film (e) are 30 and 20 times less intense than their corresponding SERS spectrum, respectively. Inset in panels (b) and (c) are $1\ \mu\text{m} \times 1\ \mu\text{m}$ AFM micrographs of the uncoated silver (z-scale: 10 nm) and gold (z-scale: 6 nm) films respectively.

The Raman spectrum of the pristine film exhibits vibrational modes in the range of $400\text{--}1600\ \text{cm}^{-1}$. The molecular structure of MEH-PPV and the assignments of selected vibrational modes are presented above Fig. 1(a).¹⁷ At the silver interface, the SERS spectrum of MEH-PPV shows reduced relative intensities of the 1110.6 and $1308.4\ \text{cm}^{-1}$ modes with respect to the bulk film indicating minimal structural or chemical variation from the bulk. In contrast, the SERS spectrum of the MEH-PPV at the gold interface exhibits two notable differences with respect to the bulk film: an extra band at $854.0\ \text{cm}^{-1}$ which is assigned to the out-of plane wagging mode of the C-H bond of the phenyl group^{21,22} and decreased relative peak intensities at 1308.4 and $1585.3\ \text{cm}^{-1}$, which are assigned to the vinyl C=C-H bend and ring C=C stretch modes, respectively. To exclude the possibility that the observed differences arise from the metal films themselves, control SERS measurements on the bare silver and gold films are shown in panels (d) and (e), respectively. The gold film shows a complete absence of structure aside from a broad background that is typical of SERS,²³ while the silver film shows weak structure that is attributed to carbon contamination that is typical of rough silver films.²⁴ This contamination signal is much weaker than the observed MEH-PPV SERS spectrum and does not significantly contribute to the reported spectra. From this comparison, we conclude that the SERS spectra for both the gold and silver interfaces reported in (b) and (c) arise from MEH-PPV within a few nanometers of the electrodes. The difference between the spectra indicates that in close proximity to the gold layer, the polymer is chemically or structurally different¹¹ than MEH-PPV both in the bulk and in the vicinity of the silver film.

To isolate the cause of the spectral differences, we explored the effect of layer deposition order as exhibited in Figure 2, which compares the SERS spectra of MEH-PPV in device configurations where the polymer is deposited on the gold (Fig. 2(a)) and where gold is deposited on top of the polymer (Fig. 2(b)). Figures 2(c) and 2(d) compare the same scenarios for a silver electrode where only a difference in the relative intensity of the $1585.3\ \text{cm}^{-1}$ mode is observed. In contrast to observations made on the Raman spectra of PEDOT,²⁰ the similarity of the spectra in (a) and (b) as well as (c) and (d) indicate that the deposition order does not significantly affect the observed SERS spectra for MEH-PPV in the vicinity of either electrode material.

We also investigated the effects of thermal annealing on the observed SERS spectra. Figure 3 compares the MEH-PPV SERS spectrum of a film annealed in the glove box at a temperature of approximately $150\ ^\circ\text{C}$ for 20 min to that of an untreated film for both silver and gold electrodes. The chosen temperature is expected to exceed the glass transition temperature of MEH-PPV, which is approximately $75\ ^\circ\text{C}$.²² The annealing process leads to the disappearance of the $854.0\ \text{cm}^{-1}$ band and modifies the relative peak intensities at 1308.4 and $1585.3\ \text{cm}^{-1}$ for gold (Figs. 3(a) and 3(b)). As a result, the SERS spectrum of the MEH-PPV/Au interface following the annealing process exhibits the same spectral features (although still with different relative intensities) as the Raman spectrum of the bulk film (Fig. 1(a)). On the other hand, the annealing process does not dramatically affect the

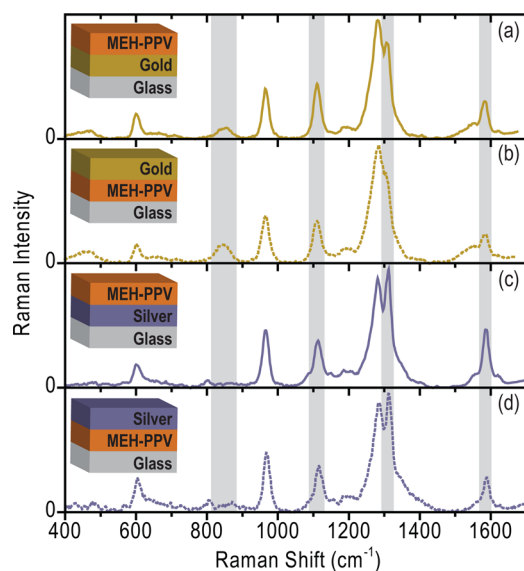


FIG. 2. Configurational dependence of SERS spectra of MEH-PPV. MEH-PPV on top of a gold film (a) and MEH-PPV sandwiched between gold and glass (b) show nearly identical SERS spectra. Likewise, MEH-PPV on top of a silver film (c) is nearly identical to the SERS spectrum of MEH-PPV sandwiched between silver and glass (d) showing only a change in the relative intensity of the 1585.3 cm^{-1} mode.

MEH-PPV/Ag SERS spectrum (Figs. 3(c) and 3(d)), again only resulting in a slightly reduced intensity of the 1585.3 cm^{-1} mode.

Thermal annealing has been widely used to modify the conformation and interfacial interactions of polymers in device-like structures.^{11,22,25,26} Using reflected Fourier transform infrared spectroscopy (FTIR), Liu *et al.* showed a similar vibrational band at $\sim 860\text{ cm}^{-1}$ in an MEH-PPV film that increased in strength after annealing.²² Combined with photoluminescence and absorption spectroscopy, they attributed the change to increased planarization of the MEH-PPV

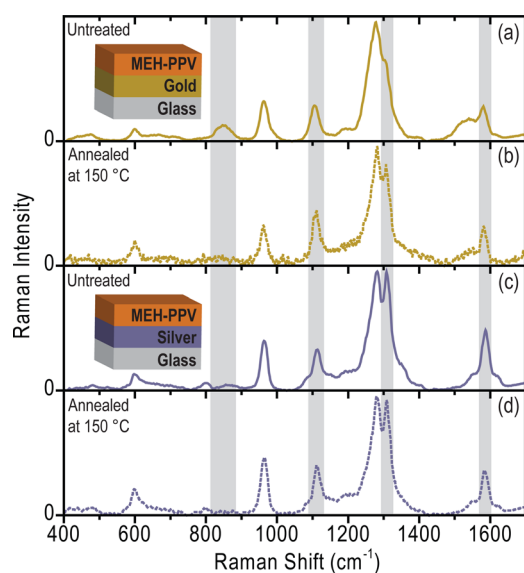


FIG. 3. Effect of thermal annealing on SERS spectra of MEH-PPV. The SERS spectrum of an untreated MEH-PPV film on gold (a) significantly changes after annealing the film at $150\text{ }^{\circ}\text{C}$ for 20 min under a nitrogen atmosphere (b). In contrast, the SERS spectrum on silver does not change (c), (d).

chains.²² A more complex scenario was recently observed by Schalnath *et al.*²¹ Using the SERS spectra of benzene molecules, an aluminum interface was shown to reduce the molecular symmetry of the benzene and amplify the 860 cm^{-1} vibrational mode. This is seemingly contradictory with the results from Liu *et al.*²² but is actually consistent, since FTIR and Raman spectroscopy typically observe mutually exclusive vibrational modes: increased intensity of a mode observed in an FTIR measurement will generally correspond to decreased intensity in a Raman measurement. Thus, in regards to our observations, we propose that the annealing process increases the planarity of phenyl rings in the polymer chains at the gold interface, thereby reducing the observed signal in SERS for the 854.0 cm^{-1} vibrational mode. Such a process is analogous to the annealing effects reported for thin films of the polymer poly(9,9-di-n-octylfluorene-alt-benzothiadiazole (F8BT)).¹¹

Surprisingly, the SERS measurements of the MEH-PPV/Ag interface suggest that the phenyl rings of the polymer are already planarized and thus annealing has very little effect on the spectra. The reduced interfacial interaction between the silver film and MEH-PPV polymer could be due to the different affinities to oxygen between the two metals. While oxygen is suspected to only physisorb on the gold surface in the molecular state,²⁷ silver is readily oxidized causing the formation of a native layer of silver oxide.²⁸ We note that even in the inert glove box environment there is sufficient oxygen present ($<2\text{ ppm}$) for this process to occur.

Finally, we probed the effect of excitation wavelength on the SERS spectra of the untreated MEH-PPV/Au and MEH-PPV/Ag interfaces. Figure 4 shows the spectra obtained with excitation at 532 nm , which is resonant with the electronic transition of MEH-PPV, as opposed to the off-resonant excitation at 785 nm . Upon resonant excitation, a significantly enhanced Raman signal of the backbone phenyl C=C stretch mode at 1585.3 cm^{-1} is observed for MEH-PPV for both gold (Fig. 4(a)) and silver (Fig. 4(b)) as compared to the off-resonant cases. Note that due to the resonant excitation, the fluorescence of the MEH-PPV was removed by fitting a second-order polynomial to the broad background. Raman scattering measurements under resonant conditions enhance the Raman modes which are coupled to the electronic transition in a process known as resonance Raman

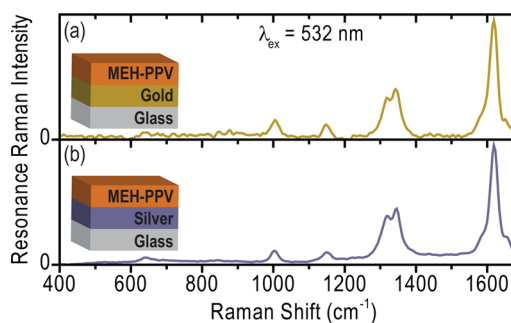


FIG. 4. SERS spectra of MEH-PPV on silver and gold films. The SERS spectra of MEH-PPV under 532 nm excitation on gold (a) and silver (b) films are nearly identical suggesting that the metal surfaces affect the vibrational modes coupled to the electronic transitions of the polymer in the same manner.

scattering (RRS).²⁹ In our case, the surface-enhanced resonance Raman scattering (SERRS) spectra at the gold and silver interfaces become identical, thus indicating that the vibrational modes coupled most strongly to the electronic transitions along the conjugated backbone of MEH-PPV are nearly identical in the presence of silver and gold, providing further evidence that the differences discussed above are not due to large conformational changes of the conjugated polymer.

We have performed a SERS investigation on the interfaces formed between MEH-PPV and nanostructured gold and silver films serving as model electrodes found in polymer-based devices. With off-resonant excitation at 785 nm, SERS from the MEH-PPV/Ag interface is very similar to the Raman spectrum obtained from a bulk film indicating minimal interfacial interactions between the polymer and the metal. The SERS spectrum from the MEH-PPV/Au interface, however, displays more marked differences: the relative intensities of the modes associated with the vinyl C=C-H bending and ring C=C stretching Raman modes are decreased, while the Raman intensity of the C-H wagging mode of the phenyl ring is dramatically increased. These differences are attributed to subtle conformational changes of the MEH-PPV at the gold interface that are then relaxed by annealing, which returns the polymer to a bulk-like conformation. Resonant excitation at 532 nm yields identical SERRS spectra for both gold and silver interfaces with MEH-PPV thus revealing that the vibrational modes that are most strongly coupled to the conjugated backbone and electronic transitions maintain similar strengths and energies in the neighborhood of both gold and silver. Such measurements provide further insight into the nature of MEH-PPV at the interface of an electrode, illustrate the capabilities of SERS and SERRS as *in situ* probes for interfaces in polymer-based devices, and demonstrate how the choice of substrate can affect SERS based measurements.

The authors thank R. Polson for technical assistance with the WITec microscope, J. M. Gerton for providing access to the AFM system, M. Navas for providing the background subtraction routine for the SERRS measurements,

and A. Thiessen for helpful discussions. Funding from the RCSA Scialog program is gratefully acknowledged.

- ¹F. So, B. Krummacher, M. K. Mathai, D. Poplavskyy, S. A. Choulis, and V.-E. Choong, *J. Appl. Phys.* **102**, 091101 (2007).
- ²H. Siringhaus, *Adv. Mater.* **17**, 2411 (2005).
- ³R. Steim, F. R. Kogler, and C. J. Brabec, *J. Mater. Chem.* **20**, 2499 (2010).
- ⁴Y. Gao, *Mater. Sci. Eng. R* **68**, 39 (2010).
- ⁵N. Koch, A. Kahn, J. Ghijsen, J.-J. Pireaux, J. Schwartz, R. Johnson, and A. Elschner, *Appl. Phys. Lett.* **82**, 70 (2003).
- ⁶H. Plank, R. Güntner, U. Scherf, and E. J. W. List, *Adv. Funct. Mater.* **17**, 1093 (2007).
- ⁷K. Tanaka, Y. Tsuchimura, K.-i. Akabori, F. Ito, and T. Nagamura, *Appl. Phys. Lett.* **89**, 061916 (2006).
- ⁸K.-H. Yim, R. Friend, and J.-S. Kim, *J. Chem. Phys.* **124**, 184706 (2006).
- ⁹H. Cheun, F. Galbrecht, B. Nehls, U. Scherf, and M. J. Winokur, *J. Mater. Sci.: Mater. Electron.* **20**, 498 (2009).
- ¹⁰H.-M. Liem, P. Etchegoin, K. S. Whitehead, and D. D. C. Bradley, *Adv. Funct. Mater.* **13**, 66 (2003).
- ¹¹J. M. Winfield, C. L. Donley, R. H. Friend, and J.-S. Kim, *J. Appl. Phys.* **107**, 024902 (2010).
- ¹²J. Kim, J. Lee, C. W. Han, N. Y. Lee, and I.-J. Chung, *Appl. Phys. Lett.* **82**, 4238 (2003).
- ¹³J.-S. Kim, P. K. H. Ho, C. E. Murphy, N. Baynes, and R. H. Friend, *Adv. Mater.* **14**, 206 (2002).
- ¹⁴S. Sakamoto, M. Okumura, Z. Zhao, and Y. Furukawa, *Chem. Phys. Lett.* **412**, 395 (2005).
- ¹⁵K. Kneipp, H. Kneipp, and J. Kneipp, *Acc. Chem. Res.* **39**, 443 (2006).
- ¹⁶M. J. Walter, J. M. Lupton, K. Becker, J. Feldmann, G. Gaefke, and S. Höger, *Phys. Rev. Lett.* **98**, 137401 (2007).
- ¹⁷Z. Wang and L. J. Rothberg, *ACS Nano* **1**, 299 (2007).
- ¹⁸N. Muraki, T. Miyamoto, and M. Yoshikawa, *Chem. Phys. Lett.* **499**, 158 (2010).
- ¹⁹E. Giorgetti, G. Margheri, T. Delrosso, S. Sottini, M. Muniz-Miranda, and M. Innocenti, *Appl. Phys. B* **79**, 603 (2004).
- ²⁰M. Stavytska-Barba and A. M. Kelley, *J. Phys. Chem. C* **114**, 6822 (2010).
- ²¹M. C. Schalnati, A. M. Hawkrige, and J. E. Pemberton, *J. Phys. Chem. C* **115**, 13717 (2011).
- ²²J. Liu, T.-F. Guo, and Y. Yang, *J. Appl. Phys.* **91**, 1595 (2002).
- ²³N. P. W. Pieczonka and R. F. Aroca, *ChemPhysChem* **6**, 2473 (2005).
- ²⁴N. J. Borys and J. M. Lupton, *J. Phys. Chem. C* **115**, 13645 (2011).
- ²⁵T. Ahn, H. Lee, and S.-H. Han, *Appl. Phys. Lett.* **80**, 392 (2002).
- ²⁶M. Kemerink, J. K. J. van Duren, A. J. J. M. van Breemen, J. Wildeman, M. M. Wienk, P. W. M. Blom, H. F. M. Schoo, and R. A. J. Janssen, *Macromolecules* **38**, 7784 (2005).
- ²⁷P. Jiang, S. Porsgaard, F. Borondics, M. Köber, A. Caballero, H. Bluhm, F. Besenbacher, and M. Salmeron, *J. Am. Chem. Soc.* **132**, 2858 (2010).
- ²⁸D. Torres, K. M. Neyman, and F. Illas, *Chem. Phys. Lett.* **429**, 86 (2006).
- ²⁹E. V. Efremov, F. Ariese, and C. Gooijer, *Anal. Chim. Acta* **606**, 119 (2008).